# Hybrid Energy Storage Configuration for High-Ratio Integration of Offshore Wind Power into Grids


Zhengyu Liu
*College of Electrical Engineering, Shanghai University of Electric Power*, Shanghai, China
2093582208@qq.com

Xiangjing Su
*Offshore Wind Power Research Institute, Shanghai University of Electric Power*, Shanghai, China
xiangjing_su@126.com

Shuai Yu
*College of Electrical Engineering, Shanghai University of Electric Power*, Shanghai, China
19186049960@163.com

Lujie Liu
*Offshore Wind Power Research Institute, Shanghai University of Electric Power*, Shanghai, China
susiellj@163.com

Zhenkun Li
*Offshore Wind Power Research Institute, Shanghai University of Electric Power*, Shanghai, China
lzk021@163.com

Yang Fu
*Offshore Wind Power Research Institute, Shanghai University of Electric Power*, Shanghai, China
mfudong@126.com



***Abstract*—To address the combined power and energy challenges posed by high proportions of offshore wind power grid integration during typhoon conditions, this paper proposes a source-grid dual-side hybrid energy storage collaborative optimization method. This approach establishes a heterogeneous architecture combining source-side lithium batteries with grid-side compressed air energy storage to manage high-frequency fluctuations and low-frequency energy demands. A multi-timescale operational mechanism based on model predictive control is designed to coordinate day-ahead scheduling with real-time smoothing. A two-layer planning model considering economic and frequency security is established, employing iterative genetic algorithm and mixed-integer programming to optimize configuration and operation. Simulation results demonstrate that this approach effectively smooths net load curves, outperforming single-storage solutions in both economic viability and technical performance, thereby providing an effective pathway for the secure integration of offshore wind power.**



**Keywords-offshore wind power, hybrid energy storage, coordinated deployment, two-layer planning**


## I. Introduction

Against the backdrop of the “dual carbon” strategy, the proportion of offshore wind power grid integration continues to rise [1-3]. However, its large-scale grid integration poses dual challenges of high-frequency power fluctuations and medium-to-long-term energy imbalance, posing a severe test to the power system's safety, stability, and flexible regulation capabilities [4].

To address these compound fluctuations, deploying hybrid energy storage systems (HESS) capable of coordinated power and energy dispatch is a key technology [5]. This technology employs a unified optimization control model to synergize the rapid response capability of source-side storage with the large-capacity support capability of grid-side storage, achieving the optimal solution for overall system operational efficiency and replacing traditional passive allocation strategies.

Scholars worldwide have extensively researched storage applications on both the source and grid sides. For source-side power smoothing, studies predominantly utilize signal decomposition algorithms to mitigate wind power output fluctuations. Reference [6] employs first-order high-pass filtering and moving averages to smooth wind power output, though phase lag effects increase energy storage requirements. Reference [7] introduces wavelet transform and an improved wavelet packet decomposition method, alleviating storage pressure by optimizing decomposition parameters. Reference [8] proposes an adaptive modal reconstruction method based on EMD, avoiding basis function dependencies while implementing power fluctuation limit constraints. While these methods smooth power, they predominantly represent passive responses lacking active interaction with grid conditions. Regarding grid-side operational control, research focuses on utilizing energy storage for ancillary services like frequency regulation or enhancing system economics and security through optimized dispatch. Reference [9] employs hybrid energy storage frequency-splitting responses to enhance frequency stability. Reference [10] reduces operational costs by establishing a centralized shared energy storage optimization framework. Reference [11] proposes a flow battery-supercapacitor coordination approach to improve system dynamic stability. However, existing studies predominantly analyze the role of source-side or grid-side energy storage in isolation, lacking joint scheduling models and coordinated control methods for source-grid dual-side energy storage. Furthermore, they fail to adequately consider the impact of extreme weather events such as typhoons.

Therefore, to address these research gaps, this paper proposes a source-grid dual-side hybrid energy storage collaborative configuration and operation method based on a two-layer optimization model. The main research includes: (1) Constructing a functionally complementary source-grid dual-side hybrid energy storage architecture to achieve coordinated control where source-side storage emphasizes rapid fluctuation mitigation and grid-side storage focuses on system


This study is sponsored by the National Key R&D Program of China “Remote monitoring and fault diagnosis technology for offshore wind power grid connected systems (2023YFB2406900)”



979-8-3315-8138-1

energy support. (2) Establishing a dual-layer planning model for hybrid energy storage that accounts for investment and operational costs alongside frequency security, enabling coordinated optimization of storage capacities on both the source and grid sides within the proposed architecture.

## II. Hybrid Energy Storage System Architecture and Coordinated Operation Mechanism

### A. Source-grid hybrid energy storage overall architecture

The overall architecture of the Source-Grid Dual-Sided Hybrid Energy Storage System (SG-HESS) proposed herein achieves a clear division of labor and collaborative relationship between the source and grid sides in terms of physical layout and functional positioning. On the source side, lithium batteries primarily address 'immediate' and "localized" power demands, whilst on the grid side, compressed air energy storage tackles 'long-term' and 'global' energy requirements.

### B. Modelling of Distributed Energy Storage Systems at Wind Farm Sites

The wind farm employs lithium-ion battery energy storage, whose operational status is characterized by the state of charge (SOC). The dynamic model is expressed as in Equation (1):

$$\mathrm{SOC_{BESS}(t)=SOC_{BESS}(t\text{-}1)\text{-}\frac{P_{BESS}(t)\cdot \Delta t}{E_{BESS}^{rated}}}\cdot\eta_{\mathrm{BESS}}(t) \quad (1)$$

where $P_{\mathrm{BESS}}(t)$ denotes the charging/discharging power at time $t$, and $\eta_{\mathrm{BESS}}(t)$ represents the charging/discharging efficiency.

BESS operation must satisfy $SOC$ constraints and power constraints, as per Equations (2) to (3):

$$\mathrm{SOC_{BESS}^{min}\le SOC_{BESS}(t)\le SOC_{BESS}^{max}} \quad (2)$$

$$-\mathrm{P_{BESS}^{ch,max}\le P_{BESS}(t)\le P_{BESS}^{dis,max}} \quad (3)$$

where $\mathrm{SOC_{BESS}^{min}}$ and $\mathrm{SOC_{BESS}^{max}}$ denote the lower and upper limits of the state of charge respectively. $P_{\mathrm{BESS}}^{\mathrm{ch,max}}$ and $P_{\mathrm{BESS}}^{\mathrm{dis,max}}$ denote the maximum charging and discharging power respectively.

### C. Modelling of Grid-Side Centralized Energy Storage Systems

The network side employs compressed air energy storage, whose large-scale energy throughput characteristics are suitable for system-level energy support. The state of energy (SOE) modelling is adopted, as shown in Equation (4):

$$\mathrm{SOE_{CAES}(t)=SOE_{CAES}(t\text{-}1)\text{-}\frac{P_{CAES}(t)\cdot \Delta t}{E_{CAES}^{rated}}}\cdot\eta_{CAES}(t) \quad (4)$$

CAES operation must satisfy SOC constraints and power constraints. As per Equations (5) to (6):

$$\mathrm{SOE_{CAES}^{min}\le SOE_{CAES}(t)\le SOE_{CAES}^{max}} \quad (5)$$

$$-\mathrm{P_{CAES}^{ch,max}\le P_{CAES}(t)\le P_{CAES}^{dis,max}} \quad (6)$$

where $\mathrm{SOE}_{\mathrm{CAES}}^{min}$ and $\mathrm{SOE}_{\mathrm{CAES}}^{max}$ denote the lower and upper limits of SOE respectively. $P_{CAES}^{ch,max}$ and $P_{\mathrm{CAES}}^{\mathrm{dis,max}}$ denote the maximum compression and power generation capacities respectively.

### D. Multi-timescale Cooperative Operation Mechanism Based on Model Predictive Control

At the daily time scale, the energy shifting strategy for grid-side $CAES$ is optimised with the objective of maximising system operational efficiency, generating a target power curve for grid integration. At the real-time scale, source-side $BESS$ employs model predictive control to track the target curve, with rolling optimisation of the objective. The specific formulae are shown in Equations (7) to (8):

$$P_{\mathrm{grid}}^{\mathrm{target}}(t)=P_{\mathrm{wind}}^{\mathrm{predict}}(t)-P_{\mathrm{CAES}}^{\mathrm{opt}}(t) \quad (7)$$

$$\min\sum_{i=1}^{N_p}\| P_{\mathrm{grid}}^{\mathrm{real}}(k+i\,|\,k)-P_{\mathrm{grid}}^{\mathrm{target}}(k+i)\|^2 \quad (8)$$

where $k$ denotes the current time step, and $Np$ represents the prediction time horizon.

## III. Construction and Solution of a Dual-Layer Capacity Optimization Model for Hybrid Energy Storage Systems

### A. Source-Grid Energy Storage Capacity Configuration

This model employs a two-layer optimization structure, with its core mechanism being bidirectional feedback between upper and lower layers. The upper planning layer uses the rated power $P_{\mathrm{BESS}}^{\mathrm{rated}}$, $P_{\mathrm{CAES}}^{\mathrm{rated}}$ and rated capacity $E_{\mathrm{BESS}}^{\mathrm{rated}}$, $E_{\mathrm{CAES}}^{\mathrm{rated}}$ of source-side lithium battery energy storage and grid-side compressed air energy storage as decision variables. Its objective function is to minimise the sum of the system's annualised total investment cost and the expected annual operating cost fed back from the lower layer model. The lower operational layer, given the configured energy storage capacities, optimises the daily scheduling and real-time control strategies for BESS and CAES. This is achieved by minimising daily operational costs for $K$ typical daily scenarios generated via K-means clustering, each assigned a probability $\pi_k$.

### B. Generation of Typical Daily Scenario Sets

To incorporate the uncertainty of annual offshore wind power output into the optimization process, the lower-level operational optimization is conducted based on the set of typical daily scenarios $\{\mu_k,\pi_k\}_{k=1}^{K}$ to K obtained through K-means clustering. The expected annual operational cost of the model is calculated by taking the probability-weighted average of the operational costs across all typical daily scenarios, as expressed by Equation (9):

$$\mathrm{C_{operation}}=\sum_{\mathrm{k=1}}^{\mathrm{K}}\pi_{\mathrm{k}}\cdot \mathrm{C_{operation,k}} \quad (9)$$

where $C_{\mathrm{operation},k}$ denotes the system's daily operating cost under the kth typical day scenario.

979-8-3315-8138-1

### C. Upper-level planning layer objective function

The objective of the upper planning layer is to minimize the system's annualized total cost $C_{\text{total}}$, as expressed by Equation (10):

$$\min C_{\text{total}} = C_{\text{investment}} + C_{\text{operation}} \tag{10}$$

where $C_{\text{operation}}$ denotes the expected annual operating cost fed back from the lower-level model. $C_{\text{investment}}$ denotes the annualized investment cost, as expressed by Equation (11):

$$\begin{aligned} C_{\text{investment}} &= (c_{p,\text{BESS}} \cdot P_{\text{BESS}}^{\text{rated}} + c_{e,\text{BESS}} \cdot E_{\text{BESS}}^{\text{rated}}) \cdot \frac{r(1+r)^N}{(1+r)^N - 1} \\ &+ (c_{p,\text{CAES}} \cdot P_{\text{CAES}}^{\text{rated}} + c_{e,\text{CAES}} \cdot E_{\text{CAES}}^{\text{rated}}) \cdot \frac{r(1+r)^N}{(1+r)^N - 1} \end{aligned} \tag{11}$$

where $c_{p,\text{BESS}}$ and $c_{e,\text{BESS}}$ denote the unit power cost and unit capacity cost of $BESS$ respectively. $c_{p,\text{CAES}}$ and $c_{e,\text{CAES}}$ denote the unit power cost and unit capacity cost of $CAES$ respectively. $r$ represents the discount rate, $N$ denotes the economic service life of the energy storage facility.

### D. Lower-level operational layer objective function

For any typical daily scenario $K$, the objective of the lower operational layer is to minimise the daily operational cost under that scenario, as shown in Equation (12):

$$\begin{aligned} \min C_{\text{operation},k} &= \sum_{t=1}^{T} \left[ c_{\text{buy}}(t) \cdot P_{\text{buy}}(t) - c_{\text{sell}}(t) P_{\text{sell}}(t) \right] \cdot \Delta t \\ &+ C_{\text{degradation}} + \lambda \cdot \sum_{t=1}^{T} \left| \Delta f(t) \right| \end{aligned} \tag{12}$$

where $c_{\text{buy}}(t)$ and $c_{\text{sell}}(t)$ denote the electricity purchase price and power during time t respectively. $P_{\text{buy}}(t)$ and $P_{\text{sell}}(t)$ denote the electricity sale price and power respectively. $C_{\text{degradation}}$ is primarily modeled as a linear or non-linear function related to throughput. $\Delta f(t)$ represents the system frequency deviation during time period t, with $\lambda$ being its penalty coefficient.

### E. Constraint settings

The optimization model constructed herein must satisfy the following physical and operational constraints, which collectively ensure the feasibility of the planning scheme and the safety of the operational strategy.

1) The rated power and capacity configuration of the energy storage system must satisfy the investment ceiling and technical requirements, as per Equations (13) to (16):

$$0 \le P_{\text{BESS}}^{\text{rated}} \le P_{\text{BESS}}^{\max}, \quad 0 \le E_{\text{BESS}} \le E_{\text{BESS}}^{\max} \tag{12}$$

$$0 \le P_{\text{CAES}}^{\text{rated}} \le P_{\text{CAES}}^{\max}, \quad 0 \le E_{\text{CAES}}^{\text{rated}} \le E_{\text{CAES}}^{\max} \tag{13}$$

$$T_{\text{BESS}}^{\min} \le \frac{E_{\text{BESS}}^{\text{rated}}}{P_{\text{BESS}}^{\text{rated}}} \le T_{\text{BESS}}^{\max}, \quad T_{\text{CAES}}^{\min} \le \frac{E_{\text{CAES}}^{\text{rated}}}{P_{\text{CAES}}^{\text{rated}}} \le T_{\text{CAES}}^{\max} \tag{14}$$

where $P_{\text{BESS}}^{\max}$, $E_{\text{BESS}}^{\max}$, $P_{\text{CAES}}^{\max}$ and $E_{\text{CAES}}^{\max}$ represent the upper limits for the permissible power and capacity configurations of lithium-ion battery and compressed air energy storage systems respectively. $T_{\text{BESS}}^{min}$ and $T_{\text{BESS}}^{max}$ denote the sustainable duration boundaries for source-side lithium battery energy storage, with a narrower range reflecting its power-oriented application characteristics. $T_{\text{CAES}}^{min}$ and $T_{\text{CAES}}^{max}$ represent the sustainable duration boundaries for grid-side compressed air energy storage, featuring a broader range to accommodate system-level energy shifting requirements.

2) The operational status of source-side lithium-ion batteries and grid-side compressed air energy storage must comply with their respective dynamic models and safety limits.

3) To ensure the safe and stable operation of the system under extreme conditions such as typhoon weather, the following key operational constraints must be satisfied, as shown in Equations (16) to (17):

$$P_{\text{wind}}(t) + P_{\text{BESS}}(t) + P_{\text{CAES}}(t) + P_{\text{buy}}(t) - P_{\text{sell}}(t) = P_{\text{load}}(t) \tag{15}$$

$$\left| P_{\text{line}}(t) \right| \le P_{\text{line}}^{\max}, \frac{\left| P_{\text{grid}}(t+\Delta t) - P_{\text{grid}}(t) \right|}{\Delta t} \le \delta_{\max} \tag{16}$$

### F. Model Solving Strategy

For the constructed two-layer optimization model, this study employs a hybrid solution strategy combining genetic algorithms with mixed-integer linear programming. Its core workflow is as follows. Upper Planning Layer: Utilizes genetic algorithms for solution. The global search capability of GAs is well-suited for handling non-convex optimization problems where capacity serves as the decision variable. Each chromosome individual represents a set of energy storage configuration schemes. Lower-level operational layer: For any capacity plan specified by the upper layer, the lower-level problem can be formulated as a mixed-integer linear programming model. This model is efficiently and accurately solved using the $CPLEX$ solver to obtain the optimal operational strategy and corresponding operational costs.

## IV. Case Study Analysis

### A. Case Configuration and Scenario Generation

This study employs a modified IEEE 30-node model, whose topology is illustrated in Figure 1. The offshore wind farms, with a total installed capacity of 1500 MW, are connected to nodes 5 and 13 respectively. Source-side lithium-ion battery energy storage is directly deployed at the wind farm grid connection points. Grid-side compressed air energy storage serves as a centralized regulation resource, deployed at nodes 2 and 14 to provide system-level energy shifting and frequency support.

This study employed K-means clustering to process s 8,760 hours of actual measurement data from the Luneng and Three Gorges wind farms in 2022, aiming to construct a set of typical operational scenarios for offshore wind power. The algorithm clustered 365 daily output curves into four representative days based on Euclidean distance as a metric, symbolizing the output characteristics of the four seasons. The occurrence probability of each day was determined by the number of days within the cluster. As evident from the net load curves for each typical day in Figure 2, spring and autumn exhibit smooth profiles with fluctuations arising from normal load variations and wind power changes. Winter displays high absolute net load values but with stable fluctuations. In contrast, the summer net load curve, simulated to reflect typhoon impacts, exhibits severe non-periodic fluctuations during midday and evening hours, resulting in frequent net load peaks and steep drops.

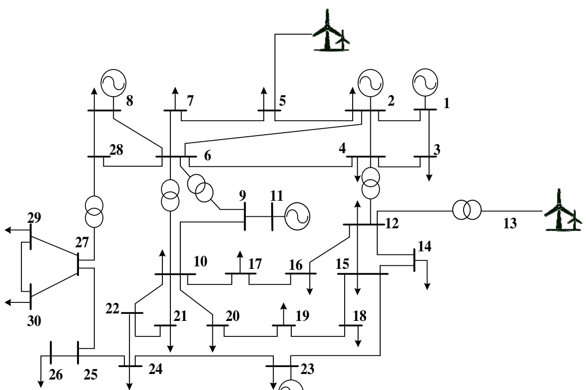

Fig. 1 Modified IEEE 30-bus System Topology

### B. *Analysis of Optimized Configuration Results for Hybrid Energy Storage Systems*

To evaluate the effectiveness of the proposed source-grid bilateral hybrid energy storage coordination configuration model, this section presents solutions and analyses based on the aforementioned case study. Firstly, Table 1 presents the optimized energy storage configuration scheme and its economic benefits. Figure 2 visually demonstrates the system's peak shaving and valley filling effects by comparing net load curves before and after energy storage deployment across four seasonal representative days. To further elucidate the synergistic operational mechanism, Figure 3 illustrates the charge-discharge power curves of source-grid bilateral energy storage during a typical summer day.

TABLE I. OPTIMIZATION CONFIGURATION RESULTS AND ECONOMIC BENEFIT ANALYSIS OF HYBRID ENERGY STORAGE SYSTEM

| Scene | Type | Capacity (MWh) | Annualized investment cost (10000/year) | Annual operating income (10000/year) |
|---|---|---|---|---|
| Spring | BESS | 150.4 | 224.1 | 698.5 |
| | CAES | 591.6 | 352.2 | 908.3 |
| Summer | BESS | 184.8 | 275.3 | 856.2 |
| | CAES | 832.2 | 770.1 | 1308.5 |
| Autumn | BESS | 156.6 | 233.3 | 735.8 |
| | CAES | 617.4 | 368.0 | 938.6 |
| Winter | BESS | 143.6 | 213.9 | 652.4 |
| | CAES | 577.2 | 344.0 | 869.7 |

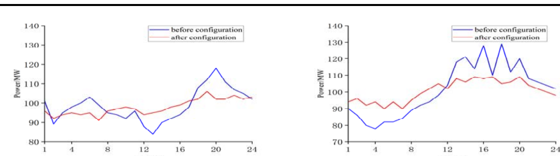


(a) Spring (b) Summer

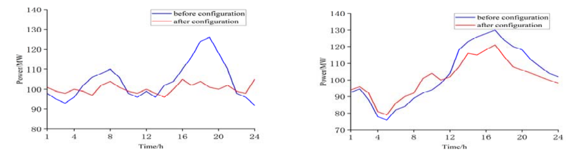


(b) autumn (d) winter

Fig.2 Comparison of Typical Daily Net Load Curves for Four Seasons

As shown in Figure 5, after deploying energy storage, the net peak-to-valley difference in load significantly decreased across all seasons, with the most pronounced effect observed in the summer scenario. The peak-to-valley difference decreased by 42.3%, while curve smoothness improved by 65.8%, effectively alleviating peak-shaving pressure and enhancing system stability. During spring and autumn, energy storage primarily smoothed normal daily fluctuations, while in winter it focused on energy time shifting, demonstrating the system's adaptive capability to different operational demands.

Figure 3 further illustrates the bilateral coordination mechanism using a typical summer day as an example: On the generation side, BESS operates frequently with rapid response, smoothing high-frequency power fluctuations during peak periods such as 08:00–12:00 and 18:00–22:00. On the grid side, CAES delivers large power amplitude with slower response, executing pre-planned energy shifting strategies to provide system-level energy support. The two systems form an effective complementarity in both temporal scale and functionality.

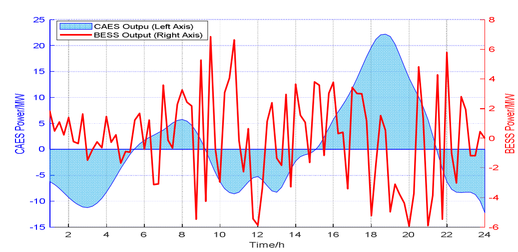


Fig.3 Typical daily two-way energy storage charge and discharge power of the source-grid in summer

### C. *Generation Multi-Solution Comparison and Validation*

To fully validate the comprehensive advantages of the proposed source-grid dual-side hybrid energy storage coordinated configuration scheme (Table 1), two comparative schemes were established under the same case study system and typical daily scenario set. Table 2 configures lithium *BESS* only at wind farm grid connection points. It employs the proposed two-layer optimization model but sets the grid-side storage capacity variable to zero, optimizing only the rated power and capacity of source-side BESS. Scheme 2 configures *CAES* only at critical grid nodes. Here, the source-side storage capacity variable is set to zero, optimizing solely the rated power and capacity of grid-side CAES.The optimal energy storage configurations and corresponding economic indicators for the three schemes are presented in Table 2. As shown in Table 2, although Scheme 1 entails the highest annualised investment cost, the synergistic operation of storage on both the generation and grid sides generates

979-8-3315-8138-1

annual operating revenues significantly exceeding those of the other schemes.

TABLE II. COMPARISON OF ENERGY STORAGE CONFIGURATION AND ECONOMY UNDER DIFFERENT SCENARIOS

| Plan | Type | Capacity (MWh) | Annualized investment cost (10000/year) | Annual operating income (10000/year) |
|---|---|---|---|---|
| Plan | BESS | 184.8 | 275.3 | 856.2 |
| one | CAES | 832.2 | 770.1 | 1308.5 |
| Plan | BESS | 431.2 | 642.9 | 1350.5 |
| two | CAES | 0 | 0 | 0 |
| Plan | BESS | 0 | 0 | 0 |
| three | CAES | 1322.4 | 905.6 | 1553.6 |

As shown in Figure 4, the selected hybrid energy storage configuration on both sides of the grid achieves peak shaving and valley filling more effectively. Scheme 1 exhibits the smoothest net load curve. While Scheme 2 mitigates some high-frequency spikes, its limited capacity prevents sustained high-power discharge during the prolonged evening peak demand. Scheme 3's net load curve fails to suppress rapid daytime power fluctuations, clearly revealing its response speed is inadequate for handling the real-time, drastic variations in wind power during typhoon conditions. In summary, from both the dual technical perspectives of peak shaving and smoothing fluctuations, the source-grid bilateral coordination scheme proposed in this paper demonstrates significantly superior technical performance compared to any single-type energy storage configuration. It provides enhanced assurance for the stability and safety of power systems under high penetration of offshore wind power.

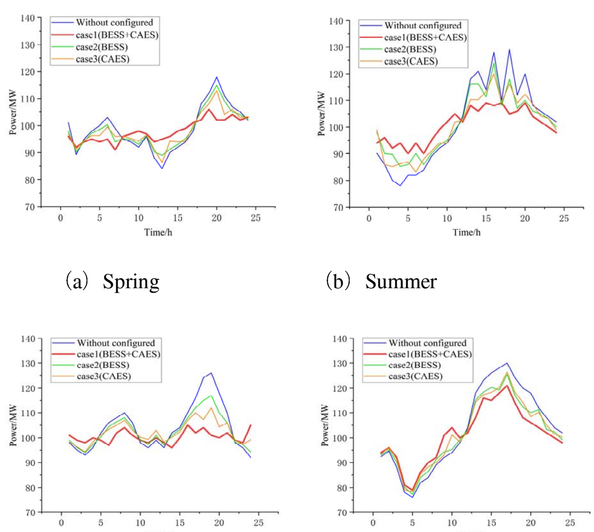


(a) Spring (b) Summer

(c) autumn (d) winter

Fig4 Daily net-load curves of four seasons under three schemes

## V. CONCLUSION

This paper addresses the challenges of high-penetration offshore wind power grid integration during typhoon weather by proposing a source-grid dual-side hybrid energy storage coordination configuration and operation method. Key conclusions are as follows:

(1) A multi-timescale coordinated operation mechanism based on model predictive control is designed, enabling active coordination between rapid power smoothing on the source side and energy shifting on the grid side, replacing traditional passive control strategies.

(2) A two-layer planning model considering economic efficiency and frequency security is established. Through iterative solution at both layers, it achieves holistic optimization of energy storage capacity allocation and operational strategies.

## ACKNOWLEDGMENT

This work is supported by National Key R&D Program of China “Remote monitoring and fault diagnosis technology for offshore wind power grid connected systems (2023YFB2406900)”.

## REFERENCES

[1] Yu Ren, Xiongfei Liu, Yi Zhu CA. The role of renewable energy investment in energy economic efficiency under the “dual carbon” policy. International Review of Economics & Finance, 2025, Vol.103:104553.

[2] Rasul Satymov CA, Dmitrii Bogdanov, Christian Breyer. Techno-economics of offshore wind power in global resolution. Applied Energy, 2025, Vol.393: 125980.

[3] Muhammad Bakr Abdelghany, Ahmed Al-Durra, Fei Gao. A Coordinated Optimal Operation of a Grid-Connected Wind-Solar Microgrid Incorporating Hybrid Energy Storage Management Systems. IEEE Transactions on Sustainable Energy, 2024, Vol.15(1): 39-51.

[4] Lu, Rui, Xiong, et al. Collaborative emergency defense strategy for offshore wind farm clusters considering the spatial-temporal characteristics of a typhoon. Power System Protection and Control, 2024, Vol.52(12): 13-24.

[5] Dan Zhou, Zhiwei Zou, Yangqing Dan,et al. An Integrated Strategy for Hybrid Energy Storage Systems to Stabilize the Frequency of the Power Grid Through Primary Frequency Regulation. Energies,2025, Vol.18(2): 246.

[6] Yu, Si, Mi,et al. Power distribution control of an island DC microgrid based on adaptive high-pass filter droop control. Power System Protection and Control, 2020, Vol. 48(18): 19-26.

[7] Wu, Xin, Li,et al. Capacity configuration method of hybrid energy storage system based on improved Wavelet packet decomposition. Acta Energiae Solaris Sinica, 2023, Vol. 44(8): 23-29.

[8] Liu, Zhengyu, Zhang,et al. State of Health Prediction for Lithium-ion Batteries Based on Empirical Mode Decomposition. Journal of Mechanical Engineering, 2024, Vol. 60(14): 272-281.

[9] Shaobo Wen, Yipeng Gong, Zhendong Zhao, et al. Power Grid Primary Frequency Control Strategy Based on Fuzzy Adaptive and State-of-Charge Self-Recovery of Flywheel–Battery Hybrid Energy Storage System. Energies, 2025, Vol.18(6): 1536.

[10] Zhu, Yidi, Xiao,et al. Centralized Shared Energy Storage Optimization Framework for AC/DC Distribution Systems with Dual-Time-Scale Coordination. Applied Sciences, 2025, Vol.15(11): 5941.

[11] Li Wang, Wang Jun-Yi Ke, Rui-Xuan Wu, et al. Stability evaluation of a grid-tied hybrid wind/PV farm joined with a hybrid energy-storage system. Sustainable Environment Research, 2023, Vol.33(1): 1-19.